

## $\rho^*$ SCALING IN RADIATIVE PLASMA REGIMES

G.F. Matthews, B. Balet, J.G. Cordey, G. Fishpool, M.G. von Hellermann, L. Horton, C. Ingesson, A. Kallenbach<sup>1</sup>, V. Parail, D. Stork, A. Taroni, G. Vlases, P. West<sup>2</sup>, K.-D. Zastrow

*JET Joint Undertaking, Abingdon, Oxfordshire, OX14 3EA*

<sup>1</sup>*Max-Planck-Institut für Plasmaphysik, EURATOM Assoc., 85478 Garching, Germany*

<sup>2</sup>*General Atomics, P.O. Box 85608, San Diego, California 92186-9784, USA*

### INTRODUCTION

The dimensionless parameter approach to energy confinement scaling studies has put the empirical approach to predicting the energy confinement in ITER on a sound physical footing. Since the plasma geometry (shape, safety factor  $q_{95}$ ), toroidal beta ( $\beta \propto nT/B^2$ ) and collisionality ( $\nu^* \propto nZ_{\text{eff}}L/T^2$ ) required by ITER can be achieved in current machines the standard approach used for type I ELMy H-modes [Cordey] is to keep these 3 dimensionless parameters fixed and scale the confinement with normalised ion gyro-radius ( $\rho^* \propto T^{0.5}/BL$ ). To perform these  $\rho^*$  scaling experiments in JET the toroidal field was varied in the range 1-2.6T. Collisionality can be kept constant by varying  $n \propto B^{4/3}$  which is achievable.

### $\rho^*$ Scaling in Radiative Regimes

Matching of the three parameters  $\rho^*$ ,  $\nu^*$  and  $\beta$  should ensure that all plasma physics phenomena, including collisional effects with Coulomb-like cross-sections are scaled correctly [Connor]. Lackner [Lackner] has shown that atomic physics effects such as radiation, charge exchange and other ion-neutral interactions of importance in the plasma edge can only be scaled when the absolute temperature,  $T$ , is also matched. In JET, detached divertor plasmas are obtained at similar values of total fractional radiated power  $f_{\text{rad}}$  and so this has been used as a closely related alternative dimensionless parameter. Using lower  $Z$  impurities (nitrogen and neon) the radiation distribution will be similar to that expected in ITER for argon. Fixing  $f_{\text{rad}}$  also avoids any confusion between changes in confinement and direct losses from within the core plasma.

### Constraints

In the JET experiments [Stork]  $q_{95}$  (3.1),  $f_{\text{rad}}$  ( $\approx 60\%$ ),  $\beta$  ( $\approx 1.2$ ) and  $Z_{\text{eff}}$  ( $\approx 3$ ) were kept constant. Fractional radiated power  $f_{\text{rad}} = P_{\text{rad, total}}/P_{\text{heat, total}}$  can be written in terms of  $Z_{\text{eff}}$  and line averaged density  $n$  by using the multi-machine  $Z_{\text{eff}}$  scaling law [Matthews] given by:  $Z_{\text{eff}} = 1 + 7 f_{\text{rad}} P_{\text{heat}}/n^2 S$ , where  $S$  the main plasma surface area.  $P_{\text{heat}}$  can then be substituted with an expression in terms of dimensionless parameters via an appropriate confinement scaling law: Gyro-Bohm  $B\tau_E \propto \rho^{*-3}$  ( $\sim$  ITER93H) or Bohm  $B\tau_E \propto \rho^{*-2}$  ( $\sim$  ITER89L). These relationships then imply that key parameters are constrained as follows:

Gyro-Bohm	$n \propto B^{6/7}$	$n/n_{\text{Greenwald}} \propto B^{-1/7}$	$v^* \propto B^{-10/7}$	$\rho^* \propto B^{-3/7}$	$P_{\text{heat}} \propto B^{12/7}$
Bohm	$n \propto B$	$n/n_{\text{Greenwald}} = \text{const.}$	$v^* \propto B^{-1}$	$\rho^* \propto B^{-1/2}$	$P_{\text{heat}} \propto B^2$

Ideally we would find a means to keep  $v^*$  constant and one possibility might be to allow  $Z_{\text{eff}}$  or  $\beta$  to vary but it turns out that the required parameter variations either do not exist or are impractical. Fortunately the  $v^*$  dependence of both the commonly used confinement scalings is rather weak ( $B\tau_{E93H} \propto v^{*-0.28}$ ,  $B\tau_{E89P} \propto v^{*-0.12}$ ) so that the failure to maintain constant  $v^*$  may have only a small effect on the results.

### Scaling of global confinement

Figure 1 shows the variation of the  $H_{\text{ITER93-H}}$  factor with  $\rho^*$  from the JET series of radiative  $\rho^*$  scaling series. Data have been restricted to pulses with  $f_{\text{rad}} > 50\%$  and multiple points have been taken from two pulses for each value of toroidal field. Also, shown are data from radiative discharges in ASDEX-Upgrade and DIII-D. All this data is consistent with a degradation with respect to the Gyro-Bohm like ITER93H scaling as  $\rho^*$  decreases. This is in contrast to the type I ELMy H-modes [Cordey] which are also shown.

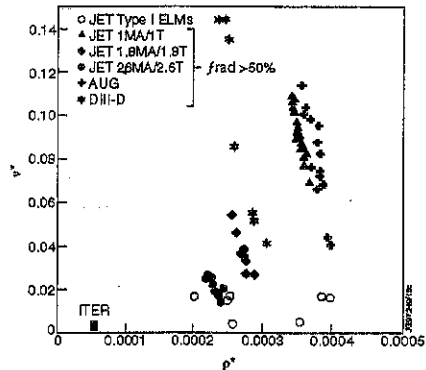
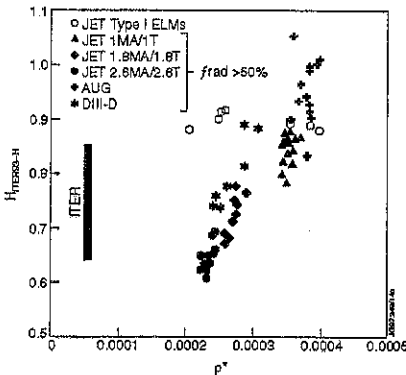


Figure 1  $H_{93}$  vs  $\rho^*$  for H-modes with  $f_{\text{rad}} > 0.5$  Figure 2  $\rho^*$  vs  $v^*$  for H-modes with  $f_{\text{rad}} > 0.5$

Figure 2 shows variation of  $\rho^*$  with  $v^*$  for the same data. Although  $v^*$  cannot be held constant in these discharges the existence of similar  $H_{\text{ITER93-H}}$  factors for widely differing  $v^*$  indicates that the confinement is weakly dependent on collisionality as is characteristic of existing scaling laws. There also appears to be no strong beta dependence.

### Local transport analysis

Local transport analysis of JET pulses using the TRANSP code shows that the thermal diffusivity of the core ( $q < 2$ ) retains its gyro-Bohm like scaling whilst the outer region is strongly degraded. Profiles of  $n_e$ ,  $T_e$ ,  $T_i$ ,  $P_e$ , total thermal pressure  $P_e + P_i$  and  $\chi_{eff}$  (dominated by  $\chi_i$ ) are shown in figures 3-8. All discharges were with  $I_p = 2.5\text{MA}$ ,  $B_T = 2.5\text{T}$  and 12MW of NB heating. A reference unfuelled type I ELMy discharge is compared with discharges seeded with nitrogen impurity. In one of these cases (37997) the density fell due to the loss in confinement but in the other (37991) strong  $D_2$  was used to maintain the density.

The observed decoupling of the core and edge confinement are not obviously consistent with confinement models in which the edge and core confinement are strongly linked [Kotschenreuter]. It is also appears different from the profile resilience reported by ASDEX-Upgrade [Suttrop] in which the core confinement appears to be set by the value at the top of the pedestal leading to self-similar  $T_e$  profiles.

In radiative discharges there may be a concern that the increase in  $\chi_{eff}$  near the edge is merely the result of direct losses which have not been correctly accounted for in the analysis. However, tomographic inversion of the bolometric data [Ingesson] shows that a majority of the radiation is emitted from outside  $q_{95}$  and as a result, the derived  $\chi_{eff}$  is very insensitive to the assumptions made about the radiation profile. Monte-Carlo calculations of the charge exchange losses coupled with bolometric evidence show that these losses are too small to influence the transport analysis and in any case are mainly located outside  $q_{95}$ .

### CONCLUSIONS

JET experiments have been described which are a first attempt at applying the dimensionless parameter approach of discharges with ITER relevant levels of radiated power and small high frequency ELMs. Global confinement scaling appears to be Bohm like which seems to result from degradation of the cross-field transport in the region outside  $q=2$ . Inside this flux surface the transport is unaffected. Rigid profile consistency does not seem to be observed in either the ion or electron temperature profiles

### REFERENCES

- Connor J.W. and Taylor J.B, *Nuclear Fusion* 17 (1977) 1047  
 Cordey G. for the JET Team, IAEA-CN-64/AP1-2, Montreal, 1996  
 Ingesson C., et al., *this proceedings*  
 Lackner K., *Comments on Plasma Physics and Controlled Fusion* 15 (1994) 359  
 Kotschenreuter M. et al., IAEA-CN-64/D1-5, Montreal, 1996  
 Matthews G.F., et al., 12th Int. Conf. on Plasma-Surface Ints., San Raphael, 1996  
 Stork D. for the JET Team, IAEA-CN-64/A1-1, Montreal, 1996  
 Suttrop W., *this conference*.

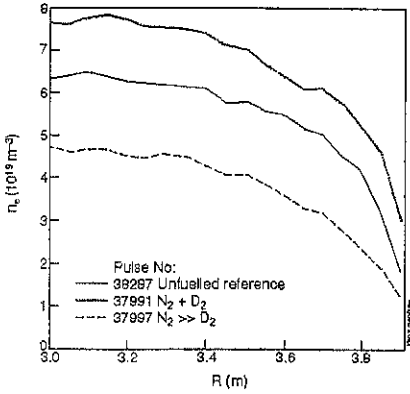


Figure 3 - Electron density profiles

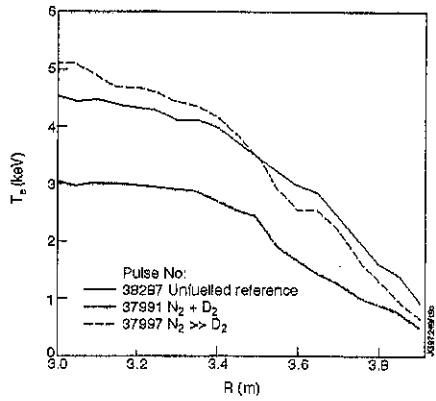


Figure 4 - Electron temperature profiles

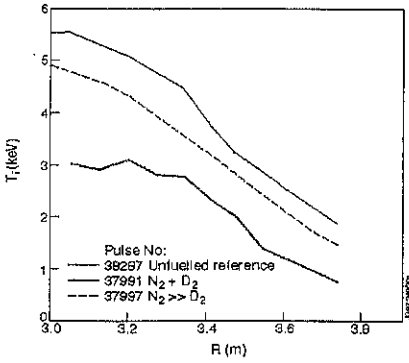


Figure 4 - Ion temperature profiles

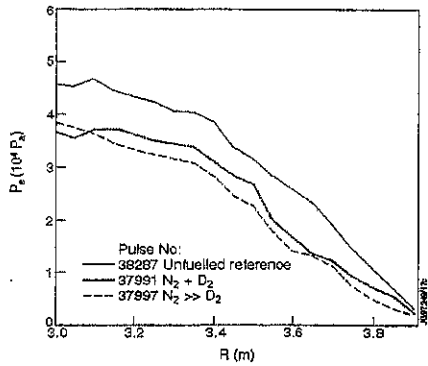


Figure 5 - Electron pressure profiles

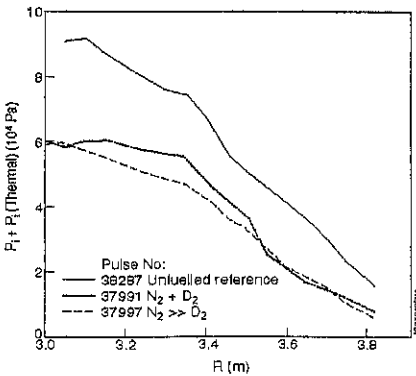


Figure 5 - Total thermal pressure profiles

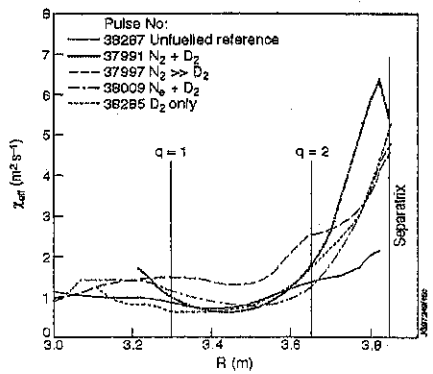


Figure 6 -  $\chi_{eff}$  profiles from TRANSP